

A High Fidelity Simulation Framework for Potential Safety Benefits Estimation of Cooperative Pedestrian Perception

Longrui Chen^{1*}, Yan Zhang^{1*}, Wenjie Jiang¹, Jiangtao Gong^{1✉}, Jiahao Shen¹, Mengdi Chu¹, Chuxuan Li¹, Yifeng Pan², Yifeng Shi², Nairui Luo², Xu Gao², Jirui Yuan¹, Guyue Zhou¹, and Yaqin Zhang¹

Abstract—This paper proposes a high-fidelity simulation framework that can estimate the potential safety benefits of vehicle-to-infrastructure (V2I) pedestrian safety strategies. This simulator can support cooperative perception algorithms in the loop by simulating the environmental conditions, traffic conditions, and pedestrian characteristics at the same time. Besides, the benefit estimation model applied in our framework can systematically quantify both the risk conflict (non-crash condition) and the severity of the pedestrian’s injuries (crash condition). An experiment was conducted in this paper that built a digital twin of a crowded urban intersection in China. The result shows that our framework is efficient for safety benefit estimation of V2I pedestrian safety strategies.

I. INTRODUCTION

Since the time of the first reported pedestrian fatality in 1899, more than 1/5 of all fatalities in road accidents worldwide are pedestrians [1]. Robust pedestrian detection and recognition are important issues for transportation. However, pedestrian safety has been a difficult issue in both developed countries and low-income countries [2]. One of the pedestrian detection challenges is that pedestrians can appear in a variety of environments with different background features and obstacles, which are more difficult to identify, predict, and protect compared with other road users by vehicle-based sensors [3].

Despite recent advances in single-vehicle perception, the individual viewpoint often results in degraded perception in long-range or occluded areas. A promising solution to this problem is through vehicle-to-everything (V2X), a cutting-edge communication technology that enables dialogue between a vehicle and other entities, including vehicle-to-vehicle (V2V) and vehicle-to-infrastructure (V2I). The efficiency of the cooperative perception provided by the V2I system heavily relies on vehicles being able to observe road conditions by detecting moving objects, especially pedestrians, in real time.

However, how to test and evaluate the safety benefits of high-fidelity simulation remains challenging. Most of current simulation framework of V2I are based on numerical simulation or traffic simulation, such as ProVerif [4], PLEXE [5], MATLAB [6], [7], SUMO [8], [9], VISSIM [10], [11], which cannot support cooperative perception in the loop. Besides, estimating the benefits of pedestrians in simulation also



Fig. 1. The real-world and simulated scenario of a crowded urban intersection using the proposed high fidelity simulation framework.

lack a quantitative evaluation model considering the overall collision rate and death rate in transportation scenario is not adequate for comparison [12].

Therefore, we design a high-fidelity simulation framework based on Carla, which can estimate the potential safety benefits of V2I pedestrian safety strategies. By simulating the environment condition, traffic condition, and pedestrian characteristics at the same time, this simulator can support the cooperative perception algorithm in the loop. Besides, the benefit estimation model applied in our framework can systematically quantify both the risk conflict (non-crash condition) and the severity of the pedestrian’s injuries (crash condition). An experiment was conducted in this paper that built a digital twin of a crowded urban intersection in China. The result shows that our framework is efficient for safety benefits estimation of V2I pedestrian safety strategies.

The main contributions of this paper are:

- 1) A high fidelity and configurable simulation framework for V2I autonomous driving simulation;
- 2) Three levels of real2sim configuration are designed and implemented in the proposed framework, including environment condition, traffic condition, and pedestrian model, to reproduce realistic scenarios in the simulation environment.
- 3) An experiment to evaluate the efficiency of the proposed framework by comparing cooperative perception and single-vehicle perception with an estimation model of potential safety benefits for pedestrians in both crash and non-crash conditions.

II. RELATED WORK

To build a state-of-the-art simulation framework for potential safety benefits estimation of cooperative pedestrian detection, we systematically review three aspects of literature: the factors that influence pedestrian safety, the evaluation model

*The two authors contribute equally to this work.

¹Institute for AI Industry Research (AIR), Tsinghua University, 10080, Haidian District, Beijing, P.R.China. secondname.firstname@air.tsinghua.edu.cn

²Baidu Inc.

for safety benefits estimation, and pedestrian detection and cooperative perception supported by V2I.

A. The Factors influencing Pedestrian Safety

Pedestrian safety is among the most important challenges in implementing measures to improve road safety [1], [2]. More than 1/5 of all fatalities in road accidents worldwide are pedestrians [13], [14], [15] and cost over one hundred billion USD per country every year [16]. From previous research [17], [18], there are three main factors obviously affect pedestrian safety: environment condition, traffic condition, and pedestrian characteristics.

For the environmental conditions, Xu et al. [19] summarised that the infrastructure of the pedestrian crossing facilities (such as physical layout, presence of refuge island or guardrail) has influential effects on pedestrian compliance to pedestrian signals. Much research [20], [21], [22] found increases in the number of traffic lanes and crosswalk length are correlated with the reduction of red light running violation rate. Yan et al. [23] other geometric designs, including the presence of central refuge, can also affect the red light running violation rate of pedestrians.

For the traffic conditions, Sun et al. [24] found that the speed of approaching vehicles affects the pedestrians underestimating the vehicle speed, which increases the collision risk. Koh et al. [25] presented that the behavior of pedestrians also depends on the volume of conflicting vehicle streams.

For the Pedestrian characteristics, the demographic characteristics (such as age and gender) of pedestrians have a significant effect on pedestrian behavior and pedestrian safety. The majority of studies indicated that the propensity of red light running of male pedestrians was higher than that of females [26], [18].

From the previous research round the pedestrian safety factors, we can see that environment condition, traffic condition and pedestrian characteristics are critical for pedestrian safety related simulation, which inspired our simulation framework.

B. Safety Evaluation for Pedestrian

Together with the development of the traffic system and pedestrian protection technology, the evaluation of pedestrian safety has been long discussed. One of the most commonly used metrics was the collision rate [27], [28], [29], [30], [31], [32], which statistically revealed the existence of a hazard. However, a single measure of absolute crash probability can ignore in-depth and underlying information, such as pedestrian injury severity and pre-crash exposure.

Multiple features of both humans and vehicles have been considered as impact factors on the severity of pedestrian injuries, such as speed, age, impact body part, hood edge, etc [33], [34]. Models have been developed to estimate the relation and sensitivity between specific factors and collision risk. Results of the logistic regression model showed elderly or younger age and crossing behavior were positively correlated with the fatal rate [35]. Eluru, Bhat, and Hensher [36] stated that age, velocity, crash location, and illumination

could be essential when evaluating severity by developing a mixed generalized ordered response model. Moreover, the collision velocity and human age have been proved to be critical factors [37], [38], [39]. Washington et al. [40] offered an S-shape risk curve, which was a function of impact speed, to evaluate the injury probability by implementing logistic regressions. This model has been further expanded to consider pedestrians' age as a variable [41].

As collision events are relatively infrequent and have a short effective observation period, traffic conflicts became a supplementary quantitative analysis before a potential hazard [42]. Surrogate safety measures (SSM) have been developed as a tool to assess conflicts by applying non-crash data [43]. Indicators including time [44], distance [45], and speed [46] were regarded as the most significant factors when considering pedestrian-vehicle interaction [47]. Amini et al. [47] proposed an SSM method combining three indicators mentioned above, which were minimum future relative distance (MD), time to minimum distance (TMD), and conflicting speed (CS). The result of the F-score validated this model as a good conflict classifier.

To perform an adequate pedestrian safety assessment, we adopted three models mentioned above as performance metrics. The analysis was conducted on pre-crash conflicts, collision probability, and post-crash severity.

C. V2I Pedestrian Detection and Simulation

Detecting dangerous pedestrians ahead of collision time is one of the primary strategies to avoid/mitigate collisions, which has drawn a lot of attention from researchers and vehicle manufacturers.

Modern vehicles are equipped with exteroceptive sensors, which are part of passive safety systems because they detect pedestrians and warn drivers or pedestrians [48]. Based on pedestrian detection, active safety features are developed, such as Pedestrian Automatic Emergency Braking (PAEB), which has also been integrated into highly automated vehicles [3]. Radar [49], [50], lidar [51], [52] and camera [53], [54] are three most frequently used sensors for pedestrian detection. However, the decrypted visibility (such as bad weather, obstacles, and complex background features) remains a challenge for detecting, tracking, and predicting by single-vehicle-based sensors [3].

Many researchers have proposed advanced perception methods based on onboard sensors, but the perception of a single autonomous vehicle is always limited by the detection range of sensors. V2I technology is designed to improve the accuracy of object detection, expand the detection range of vehicle sensors, and improve the detection of occluded objects so as to improve the safety of driving. Liu et al. [55] implemented a cooperation system fusing V2I/P2I communication and radar perception. Compared with radar, LiDAR can obtain more accurate target contour features. In [56]. The roadside camera uses a visual detector based on deep learning and maps the detection results to an HD map. Ojala et al. [57] proposed a V2I system with a mono camera as the roadside unit, running YOLOv3 on Darknet [58] to

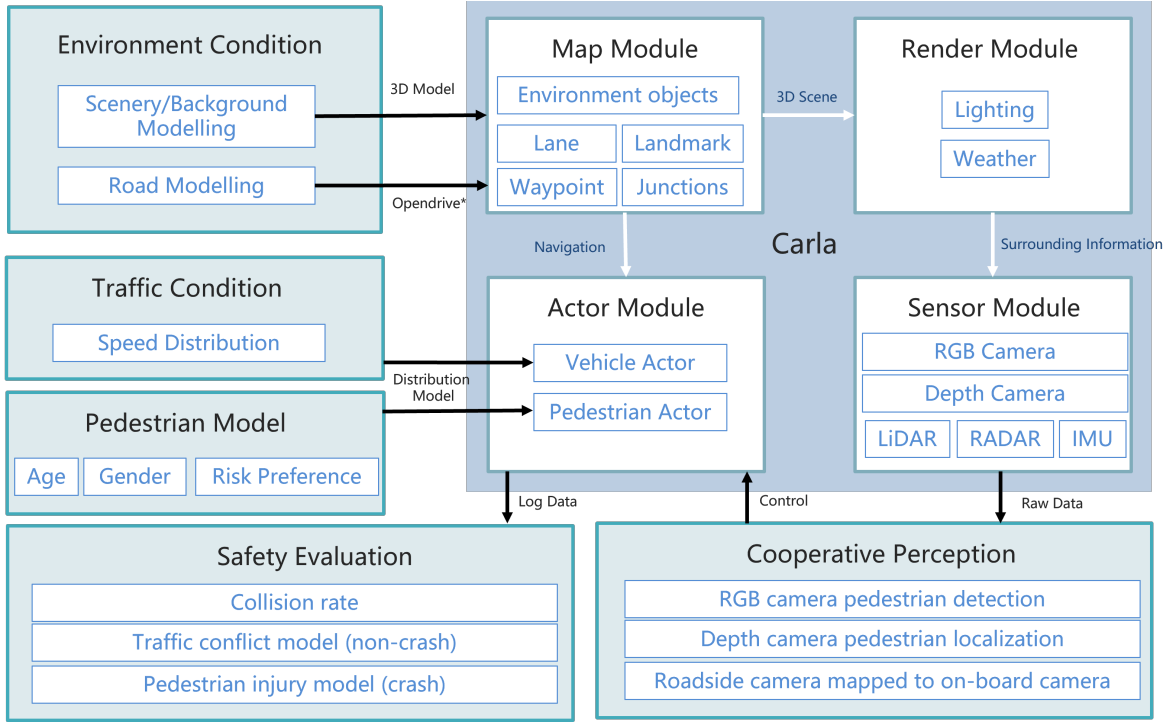


Fig. 2. The proposed high fidelity simulation framework based on Carla.

detect pedestrians, measure the distance and position of the target, and finally send the detection result to the vehicle.

Considering that V2I might be an efficient method to improve safety of pedestrian, testing based on real vehicles and real scenarios is expensive and dangerous, and methods based on numerical simulation or traffic simulation platform lack authenticity, this paper intends to build a high-fidelity simulation platform to compare the effectiveness of cooperative perception.

III. FRAMEWORK

As shown in Fig. 2, the proposed simulation framework is built based on Carla [59], consisting of five key components: environment condition, traffic condition, pedestrian model, cooperative perception, and safety evaluation.

A. Environment Condition Reconstruction

In order to support simulation in a digital twin of a realistic environment, our framework supports realistic and complex road network importing, including intersections, bridges, roundabouts, turnouts, and road markings. Both the road information (including lane, landmark, junction, and waypoint) and environment objects (including buildings, trees, traffic signs, etc.) can be reconstructed from a real road environment.

The road information based on a real-world map are created through OpenStreetMap¹ and Roadrunner². After

downloading the main road topology information from OpenStreetMap, the framework uses the roadrunner to add a lane, lane type, and landmark details. Besides, the buildings, trees, and traffic signs are modeled from pictures in Blender and then imported to Carla. As shown in Fig. 1.

B. Traffic Condition Reconstruction

In order to simulate real traffic scenarios more realistically in the simulated environment, the digital data is set referring to the traffic data distribution in the real world, including the non-intersection situation and the intersection situation, which is deployed in the form of fitted distributions.

Many studies based on real traffic data show that vehicle speed distribution follows a log-normal distribution, and vehicle headway distribution in the same lane follows a negative exponential distribution. In this paper, vehicle position distribution in different lanes is considered to be independent. Using the maximum likelihood equivalence estimation method, we made statistical analysis on nearly 30,000 real-world data, including intersection and non-intersection, and obtained the scenario distribution function under a free traffic flow state.

The negative exponential distribution of headway distribution in the same lane is:

$$P(h) = 0.1742e^{-0.1742h} \quad (1)$$

The log-normal distribution of speed distribution in non-intersection is:

$$P_{non-intersection}(v) = \frac{1}{0.4857v\sqrt{2\pi}} e^{\frac{(\ln v - 1.8304)^2}{0.4718}}, v > 0 \quad (2)$$

¹<https://www.openstreetmap.org/>

²<https://www.mathworks.com/products/roadrunner.html>

The log-normal distribution of speed distribution in an intersection is:

$$P_{intersection}(v) = \frac{1}{0.3827v\sqrt{2\pi}} e^{\frac{(\ln v - 1.5853)^2}{1.5269}}, v > 0 \quad (3)$$

The basic information of each traffic participant is defined as $\theta = (T, \dot{T})$, including the initial posture information of the participant and the micro-components of the posture information. The modifiable initial parameters of the whole scene are the complete set of initial parameters of all traffic participants, expressed as $\Theta = (T, \dot{T}) = (T_1, \dot{T}_1, T_2, \dot{T}_2, \dots, T_k, \dot{T}_k)$, i.e. $\Theta = X(0)$. For a certain scenario, firstly, the speed distribution is used to determine the initial vehicle speed. The vehicle position is determined by using the headway distribution or random uniform distribution according to the actual situation of the scenario and vehicle speed. Thus, the initial parameter distribution of a scenario can be obtained as:

$$P(\Theta) = \prod_i^k P(v_i) \prod_i^m P(x_i) \prod_i^{k-m} P(x_i) \quad (4)$$

C. Pedestrian Characteristics Modelling

In order to ensure the realism of the simulation and the validity of the result, pedestrians' behavior is modeled by three key aspects: age, gender, and risk preference. The proportions of age and gender are obtained from open databases.

Pedestrian characteristics are represented by walking speed and behavior. Walking speed is set based on the pedestrian's age and gender [60]. Limited by the sample size, the age group under 12 was eliminated. The walking speed is ranged from 1.46m/s (Young group, ages 19-30) to 1.03m/s (Older group, ages more than 60).

The risk preference is reflected in pedestrians' behavior when faced with an approaching vehicle, which is categorized into three types: 1. Pedestrian is not aware of the risk, so he/she would maintain the speed. 2. Pedestrian is aware of the risk, and he/she would speed up to pass first. 3. Pedestrian is aware of the risk, and he/she would step backward to yield.

D. Cooperative Perception of Pedestrian

The cooperative perception of pedestrians is composed of three parts, RGB camera detection, depth camera localization, and mapping between the roadside camera and the on-board camera. The RGB detection is realized by implementing YOLOV5, and the depth information is extracted from the embedding depth camera in Carla. Both of them were deployed on vehicles and roadside. In the V2I condition, the mapping procedure is achieved by transformation matrices, which are explained in detail below.

Based on the camera setup in Carla, we define the internal reference matrix as follows:

$$K = \begin{pmatrix} f_x & 0 & c_x \\ 0 & f_y & c_y \\ 0 & 0 & 1 \end{pmatrix}, \begin{cases} f_x = f_y = \frac{\text{width}}{2 \tan(\text{rad}(fov))} \\ c_x = \text{width}/2 \\ c_y = \text{height}/2 \end{cases} \quad (5)$$

Width and height are image width and height in pixels, fov is the horizontal Field Of View in degrees.

The pixels located in the bounding box are extracted with depth information, which is clustered by K-means. The center point distance of the nearest cluster is selected as the distance of pedestrians. The contour of the pedestrians is projected into the three-dimensional space of the camera coordinate system by using the internal reference matrix.

$$\begin{cases} u_I = f_x \cdot \frac{X_I}{Z_I} + c_x \\ v_I = f_y \cdot \frac{Y_I}{Z_I} + c_y \end{cases} \Rightarrow \begin{cases} X_I = (u_I - c_x) \cdot \frac{Z_I}{f_x} \\ Y_I = (v_I - c_y) \cdot \frac{Z_I}{f_y} \end{cases} \quad (6)$$

Z_I = depth is the depth value of the pixel, and $(u_I, v_I)^\top$ is the coordinate of the target point in the pixel plane of the roadside camera. X_I, Y_I, Z_I are the components of the roadside camera coordinate system, where the target point is defined as $P_I = (X_I, Y_I, Z_I)^\top$.

Finally, according to the transformation relationship between the roadside camera, the on-board camera, and the world coordinate system, the 3D points in the roadside system are mapped to the on-board system. The 3D points in the on-board system are projected to the pixel plane by using the intrinsic matrix.

$$P_V = R_V R_I^{-1} P_I \quad (7)$$

$$\begin{pmatrix} u_V \\ v_V \\ 1 \end{pmatrix} = \frac{1}{Z_V} \cdot \begin{pmatrix} f_x & 0 & c_x \\ 0 & f_y & c_y \\ 0 & 0 & 1 \end{pmatrix} \cdot \begin{pmatrix} X_V \\ Y_V \\ Z_V \end{pmatrix} \triangleq \frac{1}{z_V} K P_V \quad (8)$$

R_I and R_V are the transformation matrices from the world coordinate system to the roadside camera and the vehicle camera; $(u_V, v_V)^\top$ is the coordinates of the target point in the pixel plane of the vehicle camera; $P_V = (X_V, Y_V, Z_V)^\top$ is the 3D coordinates of the target point in the vehicle camera coordinate system.

E. Estimation Model of Safety Benefits

Pedestrian safety benefits can be accessed from the pre-crash conflict identification phase, collision rate evaluation phase, and post-crash injury severity estimation phase.

The identification of conflicts was described by three indicators as stated in [47]. The time-dependent threshold for critical situations was 1.5s, offered by [61]. Other than direct reports from Carla's recorder, the identification of collision can also be revealed from the distance-dependent indicator (MD). The speed-dependent evidence for conflicts was offered by a CS higher than 1m/s [62]. By screening with the combined criteria ($\text{conflict} \equiv ((TMD < 1.5 \vee CS > 1) \wedge MD \leq 0)$, $\text{collision} \equiv (MD \leq 0)$), events were labeled by non-conflicts, conflicts, and collisions.

After determining the nature of the events, the probability of each event occurring was calculated, which demonstrated the likelihood of pedestrians being exposed to situations with different levels of danger.

If a pedestrian-vehicle collision happens, the probability of death and severe injury can be estimated from the impact

velocity (V) and the pedestrian's age (A). By conducting multivariate logistic regressions and a 2×2 experiment, $\text{Logit}(V^2 + A)$ has been proved to have the best performance in estimating the injury rate[41]. The severe injury or death probability model of the post-collision situation used is as follows:

$$P_I = \frac{P_{\text{collision}} * e^{-2.9893 + 0.0013 * V^2 + 0.0286 * A}}{1 + e^{-2.9893 + 0.0013 * V^2 + 0.0286 * A}} \quad (9)$$

The evaluation of pedestrian safety can be used as evidence of the framework's validity and efficiency in deploying cooperative perception and simulating the environment condition, traffic condition, and pedestrian model.

IV. EVALUATION

To evaluate the proposed framework, we choose a crowded urban intersection that has a high risk for pedestrians in Beijing, China. The location and real2sim comparison is shown in Fig. 1.

A. Scenario Set-up

We design three scenarios that put pedestrians in danger based on experience and inspection. They are crossing the street in a sheltered environment, jaywalking in a sheltered environment, and crossing the street in a similarly colored environment. The first two scenarios occur in a sheltered environment that put pedestrian in danger, and the roadside camera can offer early detection and send a warning to vehicles. In the third scenario, the pedestrian is dressed in black, which is similar to the parking car near him, so the camera in the vehicle cannot detect the pedestrian in time at every moment. The schematic diagram of the three scenarios is shown in Fig. 3.

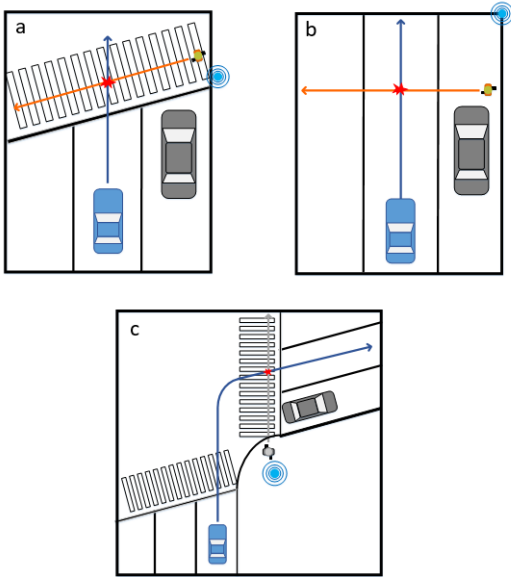


Fig. 3. Schematic diagram of Scenarios. a.Crossing. b.Jaywalking. c.Right turning. The blue circle represents the roadside camera.

A *Scenario* is defined as a specific combination of vehicle, pedestrian, and their behavior in a certain environment, such as vehicle occlusion on the second lane. The scenario is defined as $S(k, \Theta) = R, M(k), D(k), X(t)$. Where k is the number of roles in the scenario, roles refer to vehicles, pedestrians, and other objects involved. Θ is the initial parameter of each role in the scenario. R represents road information in this scenario and traffic rules that the corresponding role needs to obey. $M(k)$ is the control model of each role, including the perception and decision model. $D(k)$ is the target location for each role. The role will go to the target location according to the traffic rules based on its model. $X(t)$ is a time-varying matrix representing the basic information of all traffic participants in each frame.

When conducting the experiment, a controller will first load map information and switch perspective to an appropriate position to observe the simulation. Then, the controller will randomize initial parameters according to the scenario's rules, generate roles according to initial parameters, mount a preset perception and control model for each role, and specify the target location for each role, then the experiment starts, and the controller will start recording the experiment. When all the characters arrive at the target location or the experiment exceeds the preset time, the controller will clear all characters in the scenario and conduct the next experiment.

Each experiment will be recorded as $S(k, \Theta_i)$, each experiment will produce a result file recording collision information r_i , and global information file o_i ; The collision information file can be used for basic data analysis, while the global information file can be used for case search and culling, as well as for further data analysis.

B. Cooperative Perception Evaluation

Our collaborative perception is to project the detection results of the roadside camera onto the pixel plane of the vehicle-mounted camera, so the difference between the vehicle's own perception results and the collaborative sensing results is taken as our evaluation index. We conducted 50 experiments and extracted 20-time steps of data from each experiment. We use the roadside camera to calculate the position of the detected pedestrian and take the coordinates of the pedestrian in the real world as the ground truth and calculate the error of the measured coordinates. We obtained an average error of 0.047 meters, the variance is 2.94×10^{-4} , and the standard deviation is 0.017. We calculated the IOU of the projected bounding box of the roadside camera and the bounding box detected by the vehicle. The mean, variance, and standard deviation of test data are 0.849, 1.26×10^{-3} , and 0.035, respectively.

C. Safety Benefits Evaluation

According to the above experimental settings, experiments were carried out on the three corner cases, and each scenario was tested more than 1000 times. The experimental results are shown in table I. In every scenario, V2I with cooperative perception remarkably enhanced the safety of automated

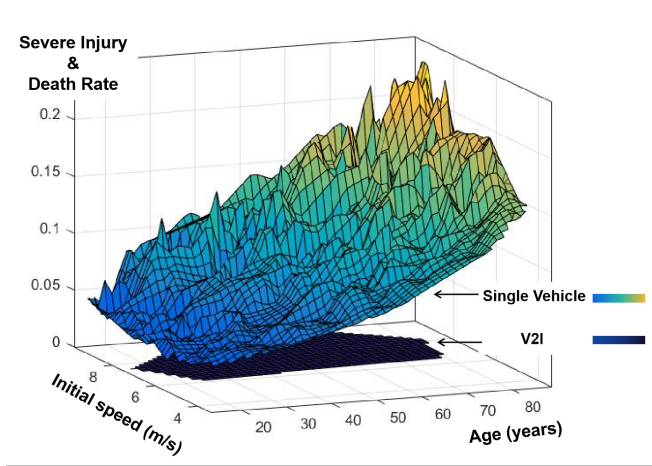


Fig. 4. The injury severity curve of single vehicle and V2I condition in the jaywalking scenario

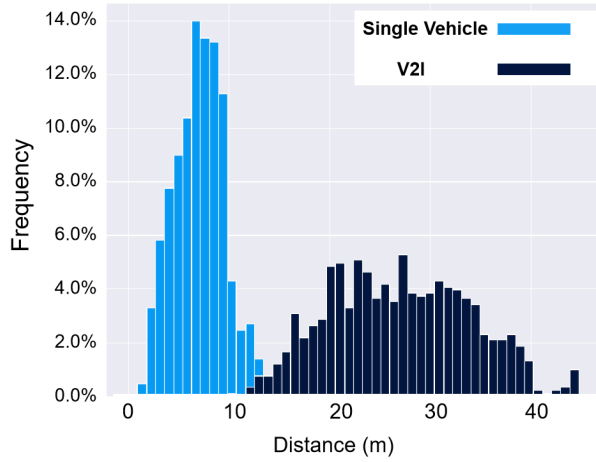


Fig. 5. Human-vehicle distance distribution when the sensor module detected the pedestrian for the first time.

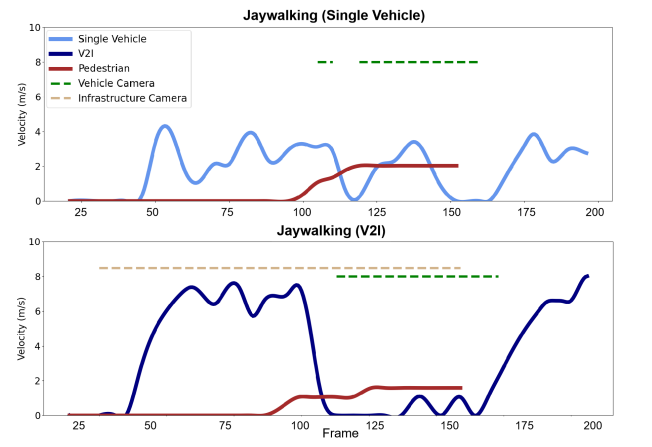


Fig. 6. A velocity-frame case visualization in jaywalking scenario. The dashed line represents the existence of on-board and roadside detection.

TABLE I
RESULTS OF EXPERIMENT IN THREE SCENARIOS.

Scenario	Condition	Conflict	Collision	Injury
Jaywalking	Single-vehicle	0.28	0.38	0.11
	V2I	0.04	0.0079	0.0028
Crossing	Single-vehicle	0.25	0.23	0.0506
	V2I	0.05	0.0075	0.00195
Right Turning	Single-vehicle	0.31	0.062	0.0017
	V2I	0.003	0	0

vehicles and pedestrians. The performance of the framework in the jaywalking scenario will be analyzed in detail below.

In the scenario of jaywalking, the safety of pedestrians is improved significantly. Both the conflict condition before the collision, the collision rate, and the severe injury rate after the collision are reduced greatly.

Fig. 4 illustrated the relation between pedestrians' age, vehicles' initial speed, and the severe injury and death rate calculated by equation (9). It can be seen that even in a critical initial state, where the vehicle had a high speed, V2I's performance still surpassed the single vehicle. The curve pattern is consistent with the above-mentioned reference, which indicates the effectiveness of the framework.

Fig. 5 demonstrates the distance between human and vehicle when the sensor first detects the pedestrian. It is noticeable that V2I can identify the pedestrian and react earlier because of the roadside sensor and cooperative perception, which results in fewer collision and conflict conditions.

A case for jaywalking scenario (Fig. 6) is illustrated by the velocity-frame graph with annotations of the cooperative perception. The pedestrian was in the middle age group with risk-seeking behavior. The V2I condition continuously detected the pedestrian while the single vehicle only detected after frame 100. The vehicle reacted in advance and avoided collision and conflict conditions even if the initial speed was higher than the other.

The above evaluation results indicate the ability of the high-fidelity simulation framework to create a digital twin of real-world intersections and provide valid results on potential safety benefits.

V. CONCLUSIONS

In this paper, we proposed a Carla-based high fidelity simulation framework that supports potential safety benefits estimation of cooperative pedestrian detection. In order to enable the cooperative perception algorithm in the loop, the proposed framework supports customizing the Map Module using real-world maps, reconstructing from real-world traffic distribution, and modeling multiple pedestrian characteristics simultaneously. Additionally, this framework integrated a model for estimating pedestrian safety benefits considering both crash and non-crash conditions. The results of evaluation experiments demonstrate the efficacy of our framework with a cooperative pedestrian detection algorithm. This framework can serve as a unified simulation and test tool for pedestrian perception algorithm benefits evaluation.

REFERENCES

- [1] W. H. Organization, *Global status report on road safety 2015*. World Health Organization, 2015.
- [2] G. Tiwari, "Progress in pedestrian safety research," *International journal of injury control and safety promotion*, vol. 27, no. 1, pp. 35–43, 2020.
- [3] T. S. Combs, L. S. Sandt, M. P. Clamann, and N. C. McDonald, "Automated vehicles and pedestrian safety: exploring the promise and limits of pedestrian detection," *American journal of preventive medicine*, vol. 56, no. 1, pp. 1–7, 2019.
- [4] V.-T. Ta and A. Dvir, "A secure road traffic congestion detection and notification concept based on v2i communications," *Vehicular Communications*, vol. 25, p. 100283, 2020.
- [5] D. Jia and D. Ngoduy, "Enhanced cooperative car-following traffic model with the combination of v2v and v2i communication," *Transportation Research Part B: Methodological*, vol. 90, pp. 172–191, 2016.
- [6] U. A. Mughal, J. Xiao, I. Ahmad, and K. Chang, "Cooperative resource management for c-v2i communications in a dense urban environment," *Vehicular Communications*, vol. 26, p. 100282, 2020.
- [7] S. D. Kumaravel and R. Ayyagari, "A decentralized signal control for non-lane-based heterogeneous traffic under v2i communication," *IEEE Transactions on Intelligent Transportation Systems*, vol. 21, no. 4, pp. 1741–1750, 2020.
- [8] Y. Xu, D. Li, and Y. Xi, "A game-based adaptive traffic signal control policy using the vehicle to infrastructure (v2i)," *IEEE Transactions on Vehicular Technology*, vol. 68, no. 10, pp. 9425–9437, 2019.
- [9] H. He, Y. Wang, R. Han, M. Han, Y. Bai, and Q. Liu, "An improved mpc-based energy management strategy for hybrid vehicles using v2v and v2i communications," *Energy*, vol. 225, p. 120273, 2021.
- [10] F. Zhang, J. Xi, and R. Langari, "Real-time energy management strategy based on velocity forecasts using v2v and v2i communications," *IEEE Transactions on Intelligent Transportation Systems*, vol. 18, no. 2, pp. 416–430, 2016.
- [11] S. Yan, J.-s. Wang, and J.-l. Wang, "Coordinated control of vehicle lane change and speed at intersection under v2x," in *2018 3rd International Conference on Mechanical, Control and Computer Engineering (ICMCCE)*. IEEE, 2018, pp. 69–73.
- [12] N. Kalra and S. M. Paddock, "Driving to safety: How many miles of driving would it take to demonstrate autonomous vehicle reliability?" *Transportation Research Part A: Policy and Practice*, vol. 94, pp. 182–193, 2016.
- [13] W. H. Organization *et al.*, "Pedestrian safety: a road safety manual for decision-makers and practitioners," 2013.
- [14] L. Wang, C. Yu, Y. Zhang, L. Luo, and G. Zhang, "An analysis of the characteristics of road traffic injuries and a prediction of fatalities in china from 1996 to 2015," *Traffic injury prevention*, vol. 19, no. 7, pp. 749–754, 2018.
- [15] K. Jamroz, M. Budzyński, A. Romanowska, J. Żukowska, J. Oskarb-ski, and W. Kustra, "Experiences and challenges in fatality reduction on polish roads," *Sustainability*, vol. 11, no. 4, p. 959, 2019.
- [16] H. Tan, F. Zhao, H. Hao, and Z. Liu, "Cost analysis of road traffic crashes in china," *International journal of injury control and safety promotion*, vol. 27, no. 3, pp. 385–391, 2020.
- [17] D. Mukherjee and S. Mitra, "A comprehensive study on identification of risk factors for fatal pedestrian crashes at urban intersections in a developing country," *Asian Transport Studies*, vol. 6, p. 100003, 2020.
- [18] D. Zhu, N. Sze, and L. Bai, "Roles of personal and environmental factors in the red light running propensity of pedestrian: Case study at the urban crosswalks," *Transportation research part F: traffic psychology and behaviour*, vol. 76, pp. 47–58, 2021.
- [19] Y. Xu, Y. Li, and F. Zhang, "Pedestrians' intention to jaywalk: Automatic or planned? a study based on a dual-process model in china," *Accident Analysis & Prevention*, vol. 50, pp. 811–819, 2013.
- [20] J. Supernak, V. Verma, I. Supernak, *et al.*, "Pedestrian countdown signals: what impact on safe crossing?" *Open journal of civil Engineering*, vol. 3, no. 03, p. 39, 2013.
- [21] Y. Yang and J. Sun, "Study on pedestrian red-time crossing behavior: integrated field observation and questionnaire data," *Transportation research record*, vol. 2393, no. 1, pp. 117–124, 2013.
- [22] K. Diependaele, "Non-compliance with pedestrian traffic lights in belgian cities," *Transportation Research Part F: Traffic Psychology and Behaviour*, vol. 67, pp. 230–241, 2019.
- [23] F. Yan, B. Li, W. Zhang, and G. Hu, "Red-light running rates at five intersections by road user in changsha, china: An observational study," *Accident Analysis & Prevention*, vol. 95, pp. 381–386, 2016.
- [24] R. Sun, X. Zhuang, C. Wu, G. Zhao, and K. Zhang, "The estimation of vehicle speed and stopping distance by pedestrians crossing streets in a naturalistic traffic environment," *Transportation research part F: traffic psychology and behaviour*, vol. 30, pp. 97–106, 2015.
- [25] P. Koh, Y. Wong, and P. Chandrasekar, "Safety evaluation of pedestrian behaviour and violations at signalised pedestrian crossings," *Safety science*, vol. 70, pp. 143–152, 2014.
- [26] S. Xie, S. Wong, T. M. Ng, and W. H. Lam, "Pedestrian crossing behavior at signalized crosswalks," *Journal of transportation engineering, Part A: Systems*, vol. 143, no. 8, p. 04017036, 2017.
- [27] C. V. Zegeer, J. Richard Stewart, H. Huang, and P. Lagerwey, "Safety effects of marked versus unmarked crosswalks at uncontrolled locations: analysis of pedestrian crashes in 30 cities," *Transportation research record*, vol. 1773, no. 1, pp. 56–68, 2001.
- [28] D. A. Quistberg, E. J. Howard, B. E. Ebel, A. V. Moudon, B. E. Saelens, P. M. Hurvitz, J. E. Curtin, and F. P. Rivara, "Multilevel models for evaluating the risk of pedestrian–motor vehicle collisions at intersections and mid-blocks," *Accident Analysis & Prevention*, vol. 84, pp. 99–111, 2015.
- [29] M. R. King, J. A. Carnegie, and R. Ewing, "Pedestrian safety through a raised median and redesigned intersections," *Transportation research record*, vol. 1828, no. 1, pp. 56–66, 2003.
- [30] W. Zheng, W. Tang, L. Jiang, and C.-W. Fu, "Se-ssd: Self-ensembling single-stage object detector from point cloud," in *Proceedings of the IEEE/CVF Conference on Computer Vision and Pattern Recognition*, 2021, pp. 14 494–14 503.
- [31] D. A. Quistberg, E. J. Howard, B. E. Ebel, A. V. Moudon, B. E. Saelens, P. M. Hurvitz, J. E. Curtin, and F. P. Rivara, "Multilevel models for evaluating the risk of pedestrian–motor vehicle collisions at intersections and mid-blocks," *Accident Analysis & Prevention*, vol. 84, pp. 99–111, 2015. [Online]. Available: <https://www.sciencedirect.com/science/article/pii/S0001457515300464>
- [32] B. Kang, "Identifying street design elements associated with vehicle-to-pedestrian collision reduction at intersections in new york city," *Accident Analysis & Prevention*, vol. 122, pp. 308–317, 2019.
- [33] S. S. Zajac and J. N. Ivan, "Factors influencing injury severity of motor vehicle–crossing pedestrian crashes in rural connecticut," *Accident Analysis & Prevention*, vol. 35, no. 3, pp. 369–379, 2003.
- [34] M. Pour-Rouholamin and H. Zhou, "Investigating the risk factors associated with pedestrian injury severity in illinois," *Journal of safety research*, vol. 57, pp. 9–17, 2016.
- [35] S. Sarkar, R. Tay, and J. D. Hunt, "Logistic regression model of risk of fatality in vehicle–pedestrian crashes on national highways in bangladesh," *Transportation research record*, vol. 2264, no. 1, pp. 128–137, 2011.
- [36] N. Eluru, C. R. Bhat, and D. A. Hensher, "A mixed generalized ordered response model for examining pedestrian and bicyclist injury severity level in traffic crashes," *Accident Analysis & Prevention*, vol. 40, no. 3, pp. 1033–1054, 2008.
- [37] R. Cuerden, D. Richards, and J. Hill, "Pedestrians and their survivability at different impact speeds," in *Proceedings of the 20th International Technical Conference on the Enhanced Safety of Vehicles, Lyon, France, Paper*, no. 07-0440, 2007.
- [38] C. Kong and J. Yang, "Logistic regression analysis of pedestrian casualty risk in passenger vehicle collisions in china," *Accident Analysis & Prevention*, vol. 42, no. 4, pp. 987–993, 2010.
- [39] K. A. Abay, "Examining pedestrian-injury severity using alternative disaggregate models," *Research in Transportation Economics*, vol. 43, no. 1, pp. 123–136, 2013.
- [40] S. Washington, M. Karlaftis, and F. Mannering, "Statistical and econometric methods for transportation data analysis," 2011.
- [41] J. Saadé, S. Cuny, M. Labrousse, E. Song, C. Chauvel, and P. Chrétien, "Pedestrian injuries and vehicles-related risk factors in car-to-pedestrian frontal collisions," in *Proceedings of the 2020 IRCOB Conference Proceedings*. IRCOB Munich, 2020, pp. 278–289.
- [42] P. Songchitruksa and A. P. Tarko, "The extreme value theory approach to safety estimation," *Accident Analysis & Prevention*, vol. 38, no. 4, pp. 811–822, 2006.
- [43] J. Hayward, *Near misses as a measure of safety at urban intersections*. Pennsylvania Transportation and Traffic Safety Center, 1971.
- [44] P. Chen, W. Zeng, G. Yu, and Y. Wang, "Surrogate safety analysis

- of pedestrian-vehicle conflict at intersections using unmanned aerial vehicle videos,” *Journal of advanced transportation*, vol. 2017, 2017.
- [45] H. D. Golakiya, R. Chauhan, and A. Dhamaniya, “Evaluating safe distance for pedestrians on urban midblock sections using trajectory plots,” *European Transport\Trasporti Europei*, vol. 75, no. 2, 2020.
 - [46] A. Svensson, *A method for analysing the traffic process in a safety perspective*. Lund Institute of Technology Sweden, 1998.
 - [47] R. E. Amini, K. Yang, and C. Antoniou, “Development of a conflict risk evaluation model to assess pedestrian safety in interaction with vehicles,” *Accident Analysis & Prevention*, vol. 175, p. 106773, 2022.
 - [48] D. Ridel, E. Rehder, M. Lauer, C. Stiller, and D. Wolf, “A literature review on the prediction of pedestrian behavior in urban scenarios,” in *2018 21st International Conference on Intelligent Transportation Systems (ITSC)*. IEEE, 2018, pp. 3105–3112.
 - [49] J. V. B. Severino, A. Zimmer, L. dos Santos Coelho, and R. Z. Freire, “Radar based pedestrian detection using support vector machine and the micro doppler effect,” in *ESANN*, 2018.
 - [50] E. Hyun, Y.-S. Jin, and J.-H. Lee, “A pedestrian detection scheme using a coherent phase difference method based on 2d range-doppler fmcw radar,” *Sensors*, vol. 16, no. 1, p. 124, 2016.
 - [51] P. J. Navarro, C. Fernandez, R. Borraz, and D. Alonso, “A machine learning approach to pedestrian detection for autonomous vehicles using high-definition 3d range data,” *Sensors*, vol. 17, no. 1, p. 18, 2016.
 - [52] K. Liu, W. Wang, and J. Wang, “Pedestrian detection with lidar point clouds based on single template matching,” *Electronics*, vol. 8, no. 7, p. 780, 2019.
 - [53] M. Saeidi and A. Ahmadi, “A novel approach for deep pedestrian detection based on changes in camera viewing angle,” *Signal, Image and Video Processing*, vol. 14, no. 6, pp. 1273–1281, 2020.
 - [54] K. M. Abughalieh and S. G. Alawneh, “Predicting pedestrian intention to cross the road,” *IEEE Access*, vol. 8, pp. 72 558–72 569, 2020.
 - [55] W. Liu, S. Muramatsu, and Y. Okubo, “Cooperation of v2i/p2i communication and roadside radar perception for the safety of vulnerable road users,” in *2018 16th International Conference on Intelligent Transportation Systems Telecommunications (ITST)*. IEEE, 2018, pp. 1–7.
 - [56] S. Masi, P. Xu, P. Bonnifait, and S.-S. Ieng, “Augmented perception with cooperative roadside vision systems for autonomous driving in complex scenarios,” in *2021 IEEE International Intelligent Transportation Systems Conference (ITSC)*. IEEE, 2021, pp. 1140–1146.
 - [57] R. Ojala, J. Vepsäläinen, J. Hanhiova, V. Hirvisalo, and K. Tammi, “Novel convolutional neural network-based roadside unit for accurate pedestrian localisation,” *IEEE Transactions on Intelligent Transportation Systems*, vol. 21, no. 9, pp. 3756–3765, 2019.
 - [58] J. Redmon, “Darknet: Open source neural networks in c,” 2013.
 - [59] A. Dosovitskiy, G. Ros, F. Codevilla, A. Lopez, and V. Koltun, “CARLA: An open urban driving simulator,” in *Proceedings of the 1st Annual Conference on Robot Learning*, 2017, pp. 1–16.
 - [60] K. Fitzpatrick, M. A. Brewer, and S. Turner, “Another look at pedestrian walking speed,” *Transportation research record*, vol. 1982, no. 1, pp. 21–29, 2006.
 - [61] C. Hydén, “The development of a method for traffic safety evaluation: The swedish traffic conflicts technique,” *Bulletin Lund Institute of Technology, Department*, no. 70, 1987.
 - [62] H. Schmidt, J. Terwilliger, D. AlAdawy, and L. Fridman, “Hacking nonverbal communication between pedestrians and vehicles in virtual reality,” *arXiv preprint arXiv:1904.01931*, 2019.